

Neutron scattering and scaling behavior in URu₂Zn₂₀ and YbFe₂Zn₂₀

C. H. Wang^{1,2}, A. D. Christianson³, J. M. Lawrence¹, E. D. Bauer², E. A. Goremychkin⁴,
A. I. Kolesnikov³, F. Trouw², F. Ronning², J. D. Thompson², M.D. Lumsden³,
N. Ni⁵, E. D. Mun⁵, S. Jia⁵, P. C. Canfield⁵, Y. Qiu^{6,7} and J. R. D. Copley⁶

¹University of California, Irvine, California 92697, USA

²Los Alamos National Laboratory, Los Alamos, NM 87545, USA

³Neutron Scattering Sciences Division, Oak Ridge National Laboratory, Oak Ridge, TN, 37831, USA

⁴Argonne National Laboratory, Argonne, IL 60439, USA

⁵Ames Laboratory, Iowa State University, Ames, IA, 50011

⁶National Institute of Standards and Technology, Gaithersburg, Maryland 20899-6102, USA

⁷Department of Materials Science and Engineering,
University of Maryland, College Park, Maryland 20742, USA

(Dated: March 3, 2022)

The dynamic susceptibility $\chi''(\Delta E)$, measured by inelastic neutron scattering measurements, shows a broad peak centered at $E_{max} = 16.5$ meV for the cubic actinide compound URu₂Zn₂₀ and 7 meV at the (1/2, 1/2, 1/2) zone boundary for the rare earth counterpart compound YbFe₂Zn₂₀. For URu₂Zn₂₀, the low temperature susceptibility and magnetic specific heat coefficient $\gamma = C_{mag}/T$ take the values $\chi = 0.011$ emu/mole and $\gamma = 190$ mJ/mole-K² at $T = 2$ K. These values are roughly three times smaller, and E_{max} is three times larger, than recently reported for the related compound UCo₂Zn₂₀, so that χ and γ scale inversely with the characteristic energy for spin fluctuations, $T_{sf} = E_{max}/k_B$. While $\chi(T)$, $C_{mag}(T)$, and E_{max} of the 4f compound YbFe₂Zn₂₀ are very well described by the Kondo impurity model, we show that the model works poorly for URu₂Zn₂₀ and UCo₂Zn₂₀, suggesting that the scaling behavior of the actinide compounds arises from spin fluctuations of *itinerant* 5f electrons.

I. INTRODUCTION

An important property of heavy fermion (HF) materials is a scaling law whereby the low temperature magnetic susceptibility χ and specific heat coefficient $\gamma = C/T$ vary as $1/T_{sf}$. Here $k_B T_{sf}$ is the spin fluctuation energy scale which can be directly observed as the maximum E_{max} in the dynamic susceptibility $\chi''(\Delta E)$, measured through inelastic neutron scattering. Such scaling receives theoretical justification¹⁻⁴ from the Anderson impurity model (AIM), where the spin fluctuation temperature T_{sf} is identified as the Kondo temperature T_K . This model assumes that fluctuations in *local* moments dominate the low temperature ground state properties of HF materials. For 4f electron rare earth HF compounds, the AIM appears to give an excellent description of much of the experimental behavior, including the temperature dependence of the magnetic contribution to the specific heat C_{mag} , the susceptibility χ , and the 4f occupation number n_f , as well as the energy dependence of the inelastic neutron scattering (INS) spectra $\chi''(\Delta E)$ of polycrystalline samples⁵. The theoretical calculations¹⁻⁴ show that these properties are highly dependent on the orbital degeneracy $N_J (= 2J + 1$ for rare earths). In particular, for large degeneracy ($N_J > 2$) both the calculated $\gamma(T)$ and $\chi(T)$ exhibit maxima at a temperature αT_K where α is a constant that depends on N_J . This kind of behavior is observed in rare earth compounds such as YbAgCu₄⁵, CeIn_{3-x}Sn_x⁶, YbCuAl⁷, and YbFe₂Zn₂₀⁸.

It is reasonable to apply the AIM, which assumes local moments, to rare earth compounds where the 4f orbitals are highly localized and hybridize only weakly with

the conduction electrons. On the other hand, in uranium compounds, the 5f orbitals are spatially extended and form dispersive bands through strong hybridization with the neighboring *s*, *p*, and *d* orbitals. Photoemission spectroscopy in 4f electron systems shows clear signals from local moment states at energies well below the Fermi level; the weak hybridization between the *f* electron and the conduction electron leads to emission near the Fermi energy ϵ_F that can be described in the context of the Anderson impurity model as a Kondo resonance⁹. In 5f electron systems, no local states are seen, but rather broad 5f band emission is observed near ϵ_F . The Anderson lattice model is sometimes employed to understand the *f*-derived band in actinide systems¹⁰ while in some systems itinerant-electron band models are employed¹¹. Hence, despite the common occurrence of scaling, we might expect differences between the uranium and the rare-earth based heavy fermion materials in the details of the thermodynamics and the spin fluctuations. Nevertheless, we have recently shown¹² that the actinide compound UCo₂Zn₂₀ exhibits a maximum in the susceptibility and a specific heat coefficient that are strikingly similar to those seen in the rare earth compound YbFe₂Zn₂₀. It is thus of interest to test whether a local moment AIM/Kondo description, which has been shown to give excellent agreement with the data for the Yb compound (see Ref. 8 and also Fig. 3 of this paper), may also be valid for 5f HF compounds.

To accomplish this, we present herein the results of INS experiments on polycrystalline URu₂Zn₂₀ together with results for the magnetic susceptibility and specific heat of single crystalline samples. We also present the INS data

on single crystal $\text{YbFe}_2\text{Zn}_{20}$. Both compounds belong to a new family of intermetallic compounds $\text{RX}_2\text{Zn}_{20}$ (R = lanthanide, Th, U; X = transition metal)^{8,13–16} which crystallize in the cubic $\text{CeCr}_2\text{Al}_{20}$ type structure ($Fd\bar{3}m$ space group)^{14,17}. In this structure, every f -atom is surrounded by 16 zinc atoms in a nearly spherical array of cubic site symmetry, which leads to small crystal field splittings. Because the R-atom content is less than 5% of the total number of atoms, and the shortest f/f spacing is ~ 6 Å, these compounds are possible candidates for studying the Anderson impurity model in periodic f electron compounds.

II. EXPERIMENT DETAILS

The crystals were grown in zinc flux^{8,12}. The magnetic susceptibility measurements were performed in a commercial superconducting quantum interference device (SQUID) magnetometer. The specific heat experiments were performed in a commercial measurement system that utilizes a relaxational (time constant) method. For $\text{URu}_2\text{Zn}_{20}$, we performed inelastic neutron scattering on a 40 gram powder sample on the low resolution medium energy chopper spectrometer (LRMECS) at IPNS, Argonne National Laboratory, on the High-Resolution Chopper Spectrometer (Pharos) at the Lujan center, LANSCE, at Los Alamos National Laboratory, and on the time-of flight Disk Chopper Spectrometer (DCS) at the NIST Center for Neutron Research. For $\text{YbFe}_2\text{Zn}_{20}$ the INS spectrum was obtained for two co-aligned crystals of total mass 8.5 grams, using the HB-3 triple-axis spectrometer at the High Flux Isotope Reactor (HFIR) at Oak Ridge National Laboratory (ORNL); the final energy was fixed at $E_f = 14.7$ meV, and the scattering plane was (H, H, L) . The data have been corrected for scattering from the empty holder but have not been normalized for absolute cross section. For the Pharos and LRMECS measurements of $\text{URu}_2\text{Zn}_{20}$, we used the non-magnetic counterpart compound $\text{ThCo}_2\text{Zn}_{20}$ to determine the scaling of the nonmagnetic scattering between low Q and high Q ; for $\text{YbFe}_2\text{Zn}_{20}$, we measured at $Q = (1.5, 1.5, 1.5)$ and $(4.5, 4.5, 4.5)$ and assumed that the phonon scattering scales as Q^2 dependence¹⁸. Assuming that the magnetic scattering scales with the Q -dependence of the $4f$ or $5f$ form factor, we subtracted the nonmagnetic component to obtain the magnetic scattering function $S_{mag}(\Delta E)$ ^{5,19,20}.

III. RESULTS AND DISCUSSION

The magnetic susceptibility $\chi(T)$ and the specific heat C/T of $\text{URu}_2\text{Zn}_{20}$ are displayed in Fig. 1 and compared to the data for $\text{UCo}_2\text{Zn}_{20}$. Fits of the data to a Curie-Weiss law (Fig. 1(a)) at high temperature give the effective moments $\mu_{eff} = 3.61 \mu_B$ for $\text{URu}_2\text{Zn}_{20}$ and $3.44 \mu_B$ for $\text{UCo}_2\text{Zn}_{20}$. The Curie-Weiss temperatures are θ

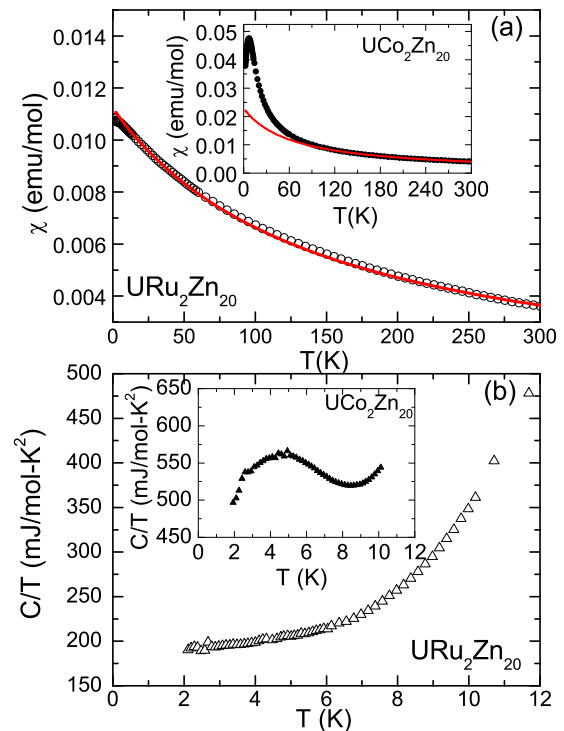


FIG. 1: (a) Magnetic susceptibility $\chi(T)$ for $\text{URu}_2\text{Zn}_{20}$. The lines are Curie-Weiss fits. (b) Specific heat C/T vs T of $\text{URu}_2\text{Zn}_{20}$. Insets: Susceptibility and specific heat of $\text{UCo}_2\text{Zn}_{20}$; the data are from Bauer *et al*¹².

= -145 K and -65 K for the Ru and Co cases, respectively. For $\text{URu}_2\text{Zn}_{20}$, the magnetic susceptibility $\chi(T)$ increases monotonically as the temperature decreases to the value $\chi(2\text{K}) \simeq 0.0111$ emu/mole. At 2 K, the susceptibility of $\text{UCo}_2\text{Zn}_{20}$ is about 0.0372 emu/mole, which is 3.3 times larger than for the Ru case. The specific heat is plotted as C/T vs T in Fig. 1 (b). For $\text{URu}_2\text{Zn}_{20}$ C/T has the magnitude $\gamma \simeq 190$ mJ/mole-K² at 2 K. At low temperature C/T follows the T^2 behavior expected for a phonon contribution, which permits the extrapolation of the Sommerfeld coefficient to the value $\gamma \simeq 188$ mJ/mole-K². From the inset to Fig. 1(b), it can be seen that for $\text{UCo}_2\text{Zn}_{20}$, $\gamma(2\text{K})$ is approximately 500 mJ/mole-K², while at $T_{max} = 4.1$ K, $\gamma = 558$ mJ/mole-K²; these values are 2.6 and 2.9 times larger than for $\text{URu}_2\text{Zn}_{20}$, respectively.

As mentioned above, the characteristic energy for spin fluctuations can be determined from the inelastic neutron scattering experiments. In Fig. 2 we plot the Q -averaged dynamic susceptibility $\chi''(\Delta E)$ of $\text{URu}_2\text{Zn}_{20}$ as a function of energy transfer ΔE . This is determined from the scattering function through the formula $S_{mag} = A(n(\Delta E) + 1)f^2(Q)\chi''(\Delta E)$, where $(n(\Delta E) + 1)$ is the Bose factor and $f^2(Q)$ is the U $5f$ form factor. Both the Pharos data and the LRMECS data for $\chi''(\Delta E)$ for $\text{URu}_2\text{Zn}_{20}$ exhibit broad peaks with peak position E_{max} at an energy transfer $\Delta E \simeq$ of or-

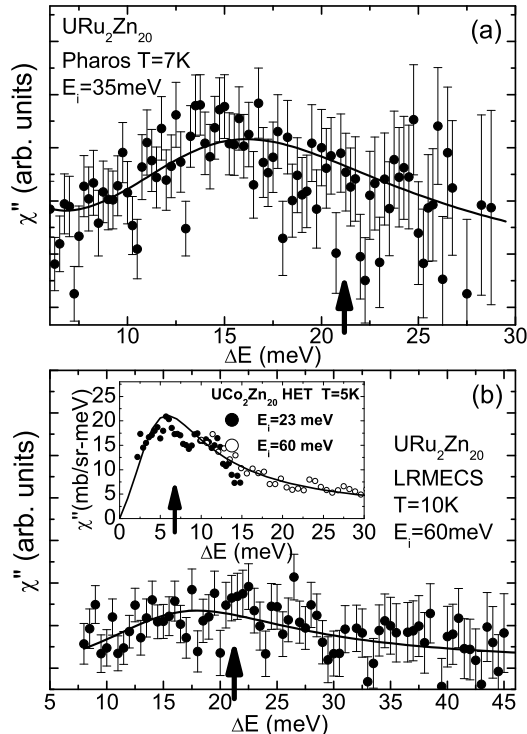


FIG. 2: Low temperature dynamic susceptibility χ'' vs ΔE of $\text{URu}_2\text{Zn}_{20}$. Error bars in all figures represent $\pm\sigma$. (a) Pharos data at $T=7$ K ($E_i = 35$ meV). (b) LRMECS data at $T=10$ K ($E_i = 60$ meV). The lines represent Lorentzian fits with $E_0=13.5$ meV \pm 1.9 meV and $\Gamma= 9.5$ meV \pm 0.6 meV. Inset: low temperature dynamic susceptibility of $\text{UCo}_2\text{Zn}_{20}$; the data are from Bauer *et al*¹². The line is a fit to a Lorentzian with $E_0=3$ meV \pm 1.2 meV and $\Gamma= 5$ meV \pm 0.4 meV. The arrows indicate the peak positions predicted by the AIM for $N_J = 10$ (See Table I).

der 16 meV. The dynamic susceptibility $\chi''(\Delta E)$ can be fit by a Lorentzian power function as $\chi''(\Delta E) = \chi''(0)\Delta E(\Gamma/\pi)/[(\Delta E - E_0)^2 + \Gamma^2]$ with the parameters $E_0 = 13.5$ meV and $\Gamma = 9.5$ meV, giving $E_{max} = 16.5$ meV. As shown in the inset to Fig. 2, for $\text{UCo}_2\text{Zn}_{20}$, $\chi''(\Delta E)$ shows a peak centered near $E_{max} = 6$ meV. Fits of this data to an inelastic Lorentzian give $E_0 = 3$ meV with $\Gamma = 5$ meV, for which $E_{max} = 5.8$ meV. We note that these values of E_{max} are nearly equal to the values of $k_B\theta$ derived from the high temperature susceptibility; i.e. the temperature scale for the suppression of the moment is identical to the energy scale of the spin fluctuation.

Given that $\gamma(2K)_{Co}/\gamma(2K)_{Ru} = 2.6$ (alternatively $\gamma(T_{max})_{Co}/\gamma(2K)_{Ru} = 2.9$), that $\chi(2K)_{Co}/\chi(2K)_{Ru} = 3.3$, and that $E_{max}(Ru)/E_{max}(Co) = 2.8$, we see that at low temperature these compounds exhibit a factor-of-three scaling of χ , γ , and E_{max} to an accuracy of about 10%.

We next examine whether such scaling arises due to

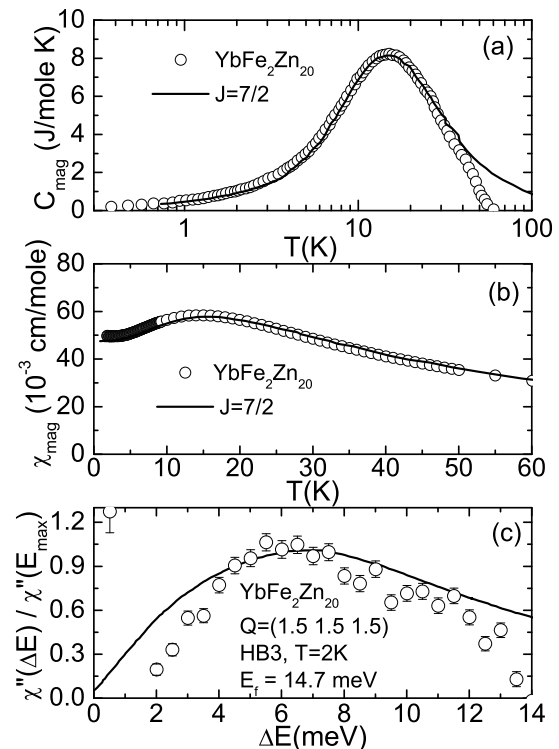


FIG. 3: (a) Specific heat $C_{mag}(T)$ (from Torikachvili *et al*⁸) and (b) magnetic susceptibility $\chi_{mag}(T)$ for $\text{YbFe}_2\text{Zn}_{20}$. (c) The dynamic susceptibility $\chi''(\Delta E)/\chi''(E_{max})$ determined at the $(3/2, 3/2, 3/2)$ zone boundary point. The lines are fits, for the $J = 7/2$ case, to Rajan's predictions for C_{mag} and χ_{mag} and to Cox's predictions for $\chi''(\Delta E)/\chi''(E_{max})$. In all three cases, there is only one common adjustable parameter T_0 , set to the value 69 K to give the best agreement with experiment.

the applicability of the AIM to these actinide compounds. Before doing so, we first check the validity of the AIM for the rare earth $4f$ compound $\text{YbFe}_2\text{Zn}_{20}$. We apply Rajan's Coqblin-Schrieffer model³, which is essentially the AIM in the Kondo limit ($n_f \simeq 1$) for large orbital degeneracy. In Fig. 3, we compare the data for $C_{mag}(T)$ and $\chi_{mag}(T)$ (where the data for $\text{LuFe}_2\text{Zn}_{20}$ has been subtracted to determine the magnetic contribution) to Rajan's predictions for the $J=7/2$ case³. In these fits, the only adjustable parameter is a scaling parameter T_0 ; we find that the value 69 K gives the best agreement with experiment.

To fit to the dynamic susceptibility $\chi''(\Delta E)$ we use the results of Cox *et al*⁴, obtained using the noncrossing approximation (NCA) to the AIM. This calculation, which was performed for the $J = 5/2$ case, gives the peak position of the dynamic susceptibility at low temperature as $E_{max} = 1.36 k_B T_0^{Cox}$ (see Fig. 5 in Cox *et al*⁴). The scaling temperature T_0^{Cox} is related to Rajan's scaling temperature T_0 via $T_0^{Cox} = T_0 / 1.15$ (see the caption of Fig. 2 in Cox *et al*⁴). Hence for the $J = 5/2$ case, we have $E_{max} = 1.18 k_B T_0$. In the absence of comparable theoretical results for other values of J , we will assume

that this relationship between T_0 and E_{max} is approximately true for the $J = 7/2$ and $9/2$ cases; the error is probably of order 20%. For $\text{YbFe}_2\text{Zn}_{20}$, we then expect $E_{max} = 7$ meV. The lineshape for $\chi''(\Delta E)/\chi''(E_{max})$ was determined from Fig. 4 in Cox *et al*⁴ using this value for E_{max} . Albeit we have only determined $\chi''(\Delta E)$ at one location in the zone, it is clear from these plots that the $N_J = 8$ AIM in the Kondo limit does an excellent job of fitting the susceptibility $\chi(T)$, magnetic specific heats C_{mag} , and characteristic energy E_{max} of this rare earth compound.

Turning now to the actinide compounds, we note that Rajan's calculations³ for a $2J+1$ Kondo impurity give the following zero-temperature limits for the specific heat, and magnetic susceptibility:

$$\gamma_0 = \pi J R / 3 T_0$$

$$\chi_0 = (2J + 1) C_J / 2\pi T_0$$

where R is the gas constant and C_J is the Curie constant. To test these scaling laws, we first note that uranium has a possible $5f^3$ state for which $J = 9/2$ and $\mu_{eff} = 3.62\mu_B$ ($C_J = 1.64$ emu K/mole) or a possible $5f^2$ state for which $J = 4$ and $\mu_{eff} = 3.58\mu_B$ ($C_J = 1.60$ emu K/mole). The high temperature Curie-Weiss fit of $\chi(T)$ for $\text{URu}_2\text{Zn}_{20}$ gives an experimental value for the Curie constant close to these free ion values. In what follows, we choose $J = 9/2$, but we note that the analysis is not significantly different for the $J = 4$ case. We estimate T_0 from the low temperature value for γ , and then determine χ_0 . To estimate E_{max} we use the above-stated rule $E_{max} = 1.18 T_0$, which as mentioned we expect to be correct here to 20%. The calculated results are listed in Table I, along with the similar results for $J = 5/2$ and $J = 1/2$.

From Table I, we can see that the expected values for χ_0 and E_{max} are closer to the experimental values for the $J = 9/2$ case than for either the $J = 5/2$ or $1/2$ cases. In Fig. 4 we compare the experimental data to the predictions (solid lines) for the temperature dependence of $\chi(T)$ and C_{mag} (where the data for the corresponding Th compound have been subtracted to determine the magnetic contribution²²) in the $J = 9/2$ case. For the energy dependence of $\chi''(\Delta E)/\chi''(E_{max})$ at low temperature, we utilize the results of Cox *et al*⁴, as outlined above. Again, there is only one adjustable parameter, T_0 , which is determined from the low temperature specific heat coefficient as equal to 208 K for the Ru case and 70 K for the Co case. The fitting is very poor in several respects. First, the expected values of T_{max} for both $\chi(T)$ and $C_{mag}(T)$ are much higher than observed in the experiment, and indeed for $\text{URu}_2\text{Zn}_{20}$ there is even no maximum in the experimental curve for $\chi(T)$. Even more significant is the fact that the experimental entropy developed below 20 K is *much* smaller than expected. Indeed the experimental entropy at 20 K is less than $R \ln 2$, which would be expected for a two-fold degeneracy ($J=1/2$). How-

ever, if we attempt to fit the data assuming $J=1/2$, we find that very small values of T_0 are required to reproduce the specific heat coefficients, and hence the characteristic energy E_{max} would disagree markedly with the experimental value (see Table I). Hence there appears to be a very serious discrepancy between the data and the Kondo model.

In our previous paper¹², we attempted to compare the data for $\text{UCo}_2\text{Zn}_{20}$ to the predictions of the AIM calculated using the NCA. The calculation assumed mixed valence between the $J = 4$ and $9/2$ states, and assumed that a large crystal field splitting (~ 200 meV) resulted in a six-fold degeneracy (effective $J = 5/2$ behavior) at low temperature. To confirm whether such a crystal field excitation is present in these compounds, we measured $\text{URu}_2\text{Zn}_{20}$ and $\text{ThCo}_2\text{Zn}_{20}$ on Pharos using large incident energies. In Fig. 5(a) we show the INS spectra for energy transfers up to $\Delta E = 550$ meV. The results exhibit no sign of crystal field excitations. We believe that a similar result will be valid for $\text{UCo}_2\text{Zn}_{20}$. Furthermore, it is clear from Table I that such an effective $J = 5/2$ approach will overestimate T_{max}^C , underestimate E_{max} and badly overestimate the entropy so that the use of the AIM to describe this compound is problematic.

Hence, while the $J = 7/2$ AIM works extremely well⁸ for the susceptibility and specific heat and also reproduces the characteristic energy E_{max} of the neutron spectrum of $\text{YbFe}_2\text{Zn}_{20}$, for these actinide compounds, the $J = 9/2$ (or $J = 4$) AIM works well only for the low temperature scaling, but very poorly for the overall temperature dependence of $\chi(T)$ and $C(T)$; in particular the theory badly overestimates the entropy. For calculations based on smaller values of N_J , the characteristic energy E_{max} is badly underestimated by the theory. These results suggest that the physics responsible for the low temperature heavy mass behavior in these actinide compounds is not that of local moments subject to the Kondo effect, as for the $4f$ electron compounds, but is that of itinerant $5f$ electrons subject to correlation enhancement. In support of this, we note that when uranium compounds such as UPd_3 exhibit local moments, then intermultiplet excitations can be observed at energies near 400 meV; no such excitation is seen for metallic compounds such as UPt_3 ²³. The lack of such excitations in the Pharos data (Fig. 5(a)) for $\text{URu}_2\text{Zn}_{20}$ gives further evidence that the $5f$ electrons are itinerant, not localized, in these compounds.

Since the peaks observed in $C_{mag}(T)$ for both the Ru and Co cases and in $\chi(T)$ for the Co case occur at a much lower temperature than the characteristic temperature E_{max}/k_B , they are very probably associated with low temperature magnetic correlations, which exist only in the vicinity of some critical wavevector Q_N , and which yield only a fraction of $R \ln 2$ for the entropy. In this regard, the behavior is similar to that of UBe_{13} or UPt_3 , where Q -dependent antiferromagnetic fluctuations occur on a much smaller energy scale (~ 1 meV for UBe_{13} and 0.2 meV for UPt_3) than the scale of the Kondo-like²⁴ fluc-

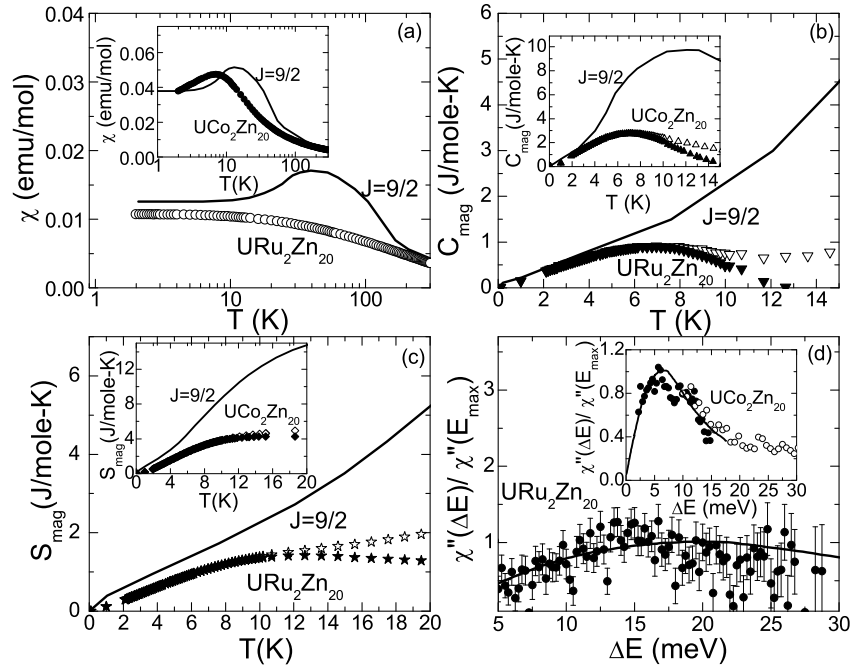


FIG. 4: (a) Magnetic susceptibility $\chi(T)$, (b) magnetic specific heat $C_{mag}(T)$, and (c) entropy $S_{mag}(T)$ for URu_2Zn_{20} ; the insets show the same quantities for UCo_2Zn_{20} ¹². The lines are fits using Rajan's predictions for $J=9/2$. The open symbols in (b) and (c) represent data corrected for the energy of the Einstein mode at 8 (7) meV in the U (Th) compounds²². (d): The dynamic susceptibility $\chi''(\Delta E)/\chi''(E_{max})$ of URu_2Zn_{20} ; the inset shows the data for UCo_2Zn_{20} . The lines are obtained using Cox's results, as explained in the text.

TABLE I: Experimental and theoretical values of key quantities for URu_2Zn_{20} and UCo_2Zn_{20} . The values for the scaling temperature T_0 are obtained using $\gamma_{2K} = 188$ mJ/mol-K² for URu_2Zn_{20} and $\gamma_{max} = 558$ mJ/mol-K² for UCo_2Zn_{20} . For $J=9/2$ and $5/2$, the Curie constant used in the calculation is the $5f^3$ free ion value while for $J=1/2$, C_J is obtained from the Curie-Weiss fit to the low temperature magnetic susceptibility.

	$T_0(K)$		$T_{max}^C(K)$		$\chi_0(\frac{emu}{mole})$		$T_{max}^X(K)$		$E_{max}(meV)$	
	Ru	Co	Ru	Co	Ru	Co	Ru	Co	Ru	Co
experiment			6.8	7.1	0.0111	0.0372		7.0	16.5	5.8
J=9/2	208	70	36.5	12.1	0.0125	0.0378	39.2	13.0	21.3	7.1
J=5/2	116	39	34.4	11.3	0.0135	0.0412	30.3	10.2	11.9	3.9
J=1/2	23	7.8	20	6.8	0.0245	0.0402			2.4	0.8

tuations (13 meV for UBe_{13} and 6 meV for UPt_3 ^{25,26}). Such antiferromagnetic fluctuations are large only in the vicinity of the wavevector Q_N and contain only a small fraction of the spectral weight compared to the Kondo-like fluctuations. Hence, it is not surprising that the polycrystalline averaged INS spectra in Fig. 5(b) shows no obvious excitation in the energy transfer range 0.1 meV to 4 meV; careful measurements on single crystals are required to reveal such low energy, low-spectral-weight Q -dependent magnetic fluctuations.

Given these considerations, we believe the characteristic INS energies of 5.8 and 16.5 meV that we have observed in UCo_2Zn_{20} and URu_2Zn_{20} represent Kondo-

like²⁴ fluctuations as observed in many uranium compounds such as UBe_{13} ²⁵, UPt_3 ²⁶ and USn_3 ²⁷. The small magnetic entropy remains a difficulty, however, even for this case. To see this, consider the scaling product $\gamma E_{max}/k_B$, which represents how the T -linear entropy is generated by the damped spin excitation centered at E_{max} . For a Kondo ion, this product takes the value $\pi JR/3$. A crude approximation would be $\gamma E_{max}/k_B = 2R \ln(2J+1)$, which might be expected to be valid even for spin fluctuations arising in an itinerant electron system; this approximation gives a similar value (~ 39) for the $J = 9/2$ case. The measured values for UCo_2Zn_{20} and URu_2Zn_{20} are in the range 33-37, very close to the

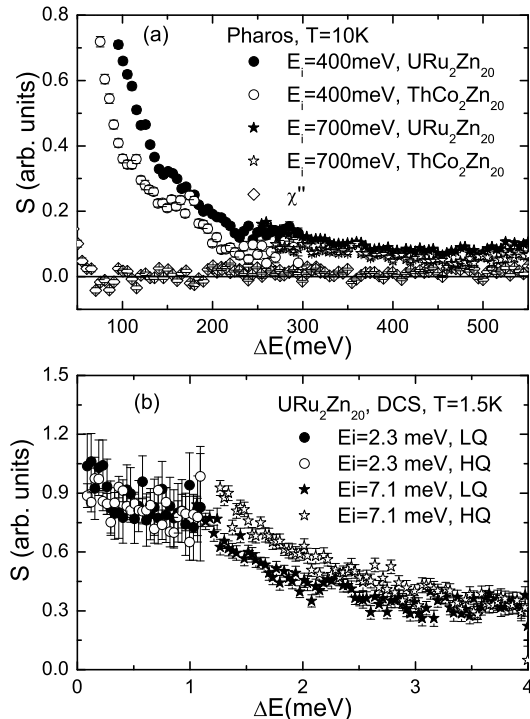


FIG. 5: (a) The INS spectra of $\text{URu}_2\text{Zn}_{20}$ and $\text{ThCo}_2\text{Zn}_{20}$ taken on Pharos with incident energies $E_i = 400$ meV and 700 meV. The diamond is the estimated magnetic scattering χ'' , obtained as described in the text. (b) The INS spectra of $\text{URu}_2\text{Zn}_{20}$ in the energy range 0.1-4 meV taken on DCS with incident energies $E_i = 2.3$ meV and 7.1 meV. The near equality of the high- Q and low- Q scattering suggests that all the scattering observed in this energy range is due to background.

expected $J = 9/2$ value. Fig. 4 indicates, however, that the compounds generate entropy in a manner that satisfies this formula only at the lowest temperatures, but then saturate above 10K. The point is that if the scaling product has the right value, then the $R \ln(2J + 1)$ entropy should continue to be generated up to temperatures of order E_{max}/k_B , much larger than 10 K for these compounds. We emphasize that this should be true even

for itinerant $5f$ electrons.

IV. CONCLUSION

The static and dynamic magnetic susceptibility and the specific heat of $\text{URu}_2\text{Zn}_{20}$ and $\text{YbFe}_2\text{Zn}_{20}$ compounds have been presented. The results show that the AIM works very well to describe the magnetic susceptibility, specific heat and dynamic susceptibility well of the compound $\text{YbFe}_2\text{Zn}_{20}$ where the $4f$ electrons are localized. In the actinide compounds $\text{URu}_2\text{Zn}_{20}$ ($\text{UCo}_2\text{Zn}_{20}$), however, the fits to the AIM temperature dependence are very poor even though the low temperature scaling behavior expected for a $J = 9/2$ Kondo impurity was observed. An associated problem is that the magnetic entropy generated by 20 K is too small compared to the expected value. These results suggest that the spin fluctuations in these actinide compounds arise from itinerant rather than localized $5f$ electrons. Antiferromagnetic fluctuations may affect the specific heat. While our neutron scattering results for a polycrystalline sample saw no signs of these fluctuations in the 0.1 to 4 meV range, they may be observable as a small spectral weight signal in single crystal experiments.

V. ACKNOWLEDGMENTS

Research at UC Irvine was supported by the U.S. Department of Energy, Office of Basic Energy Sciences, Division of Materials Sciences and Engineering under Award DE-FG02-03ER46036. Work at ORNL was supported by the Scientific User Facilities Division Office of Basic Energy Sciences (BES), DOE. Work at ANL was supported by DOE-BES under contract DE-AC02-06CH11357. Work at the Ames Laboratory was supported by the DOE-BES under Contract No. DE-AC02-07CH11358. Work at Los Alamos, including work performed at the Los Alamos Neutron Science Center, was also supported by the DOE-BES. Work at NIST utilized facilities supported in part by the National Science Foundation under Agreement NO. DMR-0454672.

¹ A. C. Hewson, *The Kondo Problem to Heavy Fermions* (Cambridge University Press), 1997.

² N. E. Bickers, D. L. Cox, and J. W. Wilkins, *Phys. Rev. B* **36**, 2036 (1987).

³ V. T. Rajan, *Phys. Rev. Lett.* **51**, 308 (1983).

⁴ D. L. Cox, N. E. Bickers, and J. W. Wilkins, *J. Magn. Magn. Matter.* **54**, 333 (1986).

⁵ J. M. Lawrence, P. S. Riseborough, C. H. Booth, J. L. Sarrao, J. D. Thompson, and R. Osborn, *Phys. Rev. B* **63**, 054427 (2001).

⁶ J. M. Lawrence, *Phys. Rev. B* **20**, 3770 (1979).

⁷ D. M. Newns and A. C. Hewson, in *Valence Fluctuations*

in Solids, L. M. Falicov, W. Hanke, and M. B. Maple, editors, North Holland, 1981, p. 27.

⁸ M. S. Torikachvili, S. Jia, E. D. Mun, S. T. Hannahs, R. C. Black, W. K. Neils, Dinesh Martien, S. L. BudŠko, and P. C. Canfield, *PNAS* **104**, 9960 (2007).

⁹ A. Koitzsch, S. V. Borisenko, D. Inosov, J. Geck, V. B. Zabolotnyy, H. Shiozawa, M. Knupfer, J. Fink, B. Buchner, E. D. Bauer, J. L. Sarrao, and R. Follath, *Phys. Rev. B* **77**, 155128 (2008).

¹⁰ J.D. Denlinger, G.-H. Gweon, J.W. Allen, C.G. Olson, M.B. Maple, J.L. Sarrao, P.E. Armstrong, Z. Fisk, H. Yamagami, *J. Electron Spectrosc. Relat. Phenom.* **117-118**,

- 347 (2001).
- ¹¹ E. Guziewicz, T. Durakiewicz, M. T. Butterfield, C. G. Olson, J. J. Joyce, A. J. Arko, J. L. Sarrao, D. P. Moore, and L. Morales, *Phys. Rev. B* **69**, 045102 (2004); T. Durakiewicz, C. D. Batista, J. D. Thompson, C. G. Olson, J. J. Joyce, G. H. Lander, J. E. Gubernatis, E. Guziewicz, M. T. Butterfield, A. J. Arko, J. Bonca, K. Mattenberger, and O. Vogt, *Phys. Rev. Lett.* **93**, 267205 (2004).
 - ¹² E. D. Bauer, C. Wang, V. R. Fanelli, J. M. Lawrence, E. A. Goremychkin, N. R. de Souza, F. Ronning, J. D. Thompson, A. V. Silhanek, V. Vildosola, A. M. Lobos, A. A. Aligia, S. Bobev, and J. L. Sarrao, *Phys. Rev. B* **78**, 115120 (2008).
 - ¹³ E. D. Bauer, J. D. Thompson, J. L. Sarrao, and M. F. Hundley, *J. Magn. Magn. Mater.* **310**, 449 (2007).
 - ¹⁴ Verena M. T. Thiede, Wolfgang Jeitschko, Sabine Niemann, Thomas Ebel, *J. Alloys Compd.* **267**, 23 (1998).
 - ¹⁵ A. P. Goncalves, J.C. Waerenborgh, A. Amaro, M. Godinho, M. Almeida, *J. Alloys Compd.* **271**, 456 (1998).
 - ¹⁶ S. Jia, S. L. Bud'ko, G. D. Samolyuk, and P. C. Canfield, *Nature Physics* **3**, 335 (2007).
 - ¹⁷ S. Niemann, and W. Jeitschko, *J Solid State Chem.* **114**, 337 (1995).
 - ¹⁸ Although the coherent approximation (Q^2 dependence) is not expected to be valid for a single crystal, the resulting magnetic scattering in this single crystal is identical to that obtained in polycrystals (A. D. Christianson et al. unpublished data) where the approximation is valid. This may reflect the very complex unit cell for this compound which includes 184 atoms/unit cell.
 - ¹⁹ A. P. Murani, *Phys. Rev. B* **28**, 2308 (1983).
 - ²⁰ E. A. Goremychkin, R. Osborn, *Phys. Rev. B* **47**, 14280 (1993).
 - ²¹ J. M. Lawrence, P. S. Riseborough, C. H. Booth, J. L. Sarrao, J. D. Thompson and R. Osborn, *Phys. Rev. B* **63**, 054427 (2001).
 - ²² In our recent paper¹² we found that the optic phonon peak seen at 8 meV in $\text{UCo}_2\text{Zn}_{20}$ occurs at 7 meV in $\text{ThCo}_2\text{Zn}_{20}$. This shift arises from the contribution of the $5f$ electrons to the crystal bonding. The specific heat for this optic mode will thus be larger for the latter compound, causing an error at low temperature in the magnetic specific heat obtained by the U - Th subtraction. The open symbols in Fig. 4 have corrected for this effect, assuming Einstein modes with three degrees of freedom. The effect is small for $T < 20\text{K}$, hence the small magnetic entropy cannot be explained on this basis.
 - ²³ M. J. Bull, K. A. McEwen, R. Osborn and R. S. Eccleston, *Physica B*, **224**, 175-177 (1996).
 - ²⁴ We call these fluctuations "Kondo-like" because they represent excitation of the magnetic moment at temperatures $T > E_{max}/k_B$, but where the moment arises from itinerant rather than local electrons.
 - ²⁵ S. Coad, A. Hiess, D. F. McMorrow, G. H. Lander, G. Aeppli, Z. Fisk, G. R. Stewart, S. M. Hayden, and H. A. Mook, *Physica B* **276-278**, 764 (2000).
 - ²⁶ A. I. Goldman, G. Shirane, G. Aeppli, E. Bucher and J. Hufnagl, *Phys. Rev. B* **36**, 8523 (1987); G. Aeppli, E. Bucher, C. Broholm, J. K. Kjems, J. Baumann and J. Hufnagl, *Phys. Rev. Lett.* **60**, 615 (1988).
 - ²⁷ M. Loewenhaupt, C. K. Loong, *Phys. Rev. B* **41**, 9294 (1990).